Pure Appl. Chem., Vol. 82, No. 10, pp. 1901–1917, 2010.
doi:10.1351/PAC-CON-09-10-22

Hydrated metal ions in aqueous solution: How regular are their structures?

Ingmar Persson

Department of Chemistry, Swedish University of Agricultural Sciences, P.O. Box 7015, SE-750 07 Uppsala, Sweden

Abstract: The hydration reaction is defined as the transfer of an ion or neutral chemical species from the gaseous phase into water, $M^{n+}(g) \rightarrow M^{n+}(aq)$. In this process, water molecules bind to metal ions through ion-dipole bonds of mainly electrostatic character. The hydration reaction is always strongly exothermic with increasing heat of hydration with increasing charge density of the ion. The structures of the hydrated metal ions in aqueous solution display a variety of configurations depending on the size and electronic properties of the metal ion. The basic configurations of hydrated metal ions in aqueous solution are tetrahedral, octahedral, square antiprismatic, and tricapped trigonal prismatic. This paper gives an overview of the structures of hydrated metal ions in aqueous solution with special emphasis on those with a non-regular coordination figure. Metal ions without d-electrons in the valance shell form regular aqua complexes with a coordination figure, allowing a maximum number of water molecules to be clustered around the metal ion. This number is dependent on the ratio of the metal ion radius to the atomic radius of oxygen in a coordinated water molecule (1.34 Å). The lighter lanthanoid(III) ions have a regular tricapped trigonal prismatic configuration with the M–O distance to the capping water molecules somewhat longer than to the prismatic ones. However, with increasing atomic number of the lanthanoid(III) ions, an increasing distortion of the capping water molecules is observed, resulting in a partial loss of water molecules in the capping positions for the heaviest lanthanoids. Metal ions with d^4 and d^9 valance shell electron configuration, as chromium(II) and copper(II), respectively, have Jahn–Teller distorted aqua complexes. Metal ions with low charge and ability to form strong covalent bonds, as silver(I), mercury(II), palladium(II), and platinum(II), often display distorted coordination figures due to the second-order Jahn–Teller effect. Metal ions with $d^{10}s^2$ valence shell electron configuration may have a stereochemically active lone electron pair (hemi-directed complexes) or an inactive one (holo-directed). The hydrated tin(II), lead(II), and thallium(I) ions are hemi-directed in aqueous solution, while the hydrated bismuth(III) ion is holo-directed. The structures of the hydrated cationic oxo-metal ions are reported as well.

Keywords: coordination chemistry; coordination geometry; hydration; metal ions; water.

*Paper based on a presentation at the 31st International Conference on Solution Chemistry (ICSC-31), 21–25 August 2009, Innsbruck, Austria. Other presentations are published in this issue, pp. 1855–1973.

INTRODUCTION

This paper aims to give an overview of the structures of hydrated metal ions, especially the first hydration shell, in different parts of the periodic table, and point out the areas in the periodic table where it is expected to find metal ions with specific physical-chemical and structural properties based on mainly experimental structural studies in aqueous solution, sometimes supported by crystal structures. Experimental hydration dynamics and theoretical simulations of hydrated metal ions will not be presented or discussed as it lies outside the scope of this paper even though they give a very important contribution to the understanding of the physical-chemical properties of hydrated metal ions in aqueous solution.

HYDRATION OF METAL IONS

The hydration reaction is defined as the transfer of an ion or a neutral chemical species from the gaseous phase into water; for metal ions $M^{n+}(g) \rightarrow M^{n+}(aq)$. At this process, water molecules bind to metal ions through ion-dipole bonds of mainly electrostatic character and to anions through mainly hydrogen bonds. The hydration reaction is always strongly exothermic with increasing heats of hydration with increasing charge density of the ion, with a value of the heat of hydration of metal ions of about $\Delta_{hydr}H = -974 \cdot Z^2/d_{M-O}$ (kJ mol^{-1}); Z = charge of ion and d_{M-O} = mean M–O bond distance in Å of the hydrated metal ion in aqueous solution, Fig. 1. The entropy term of the hydration reaction has a small negative value, and thereby the Gibbs energy of hydration is slightly less negative than the corresponding heat of hydration [1,2].

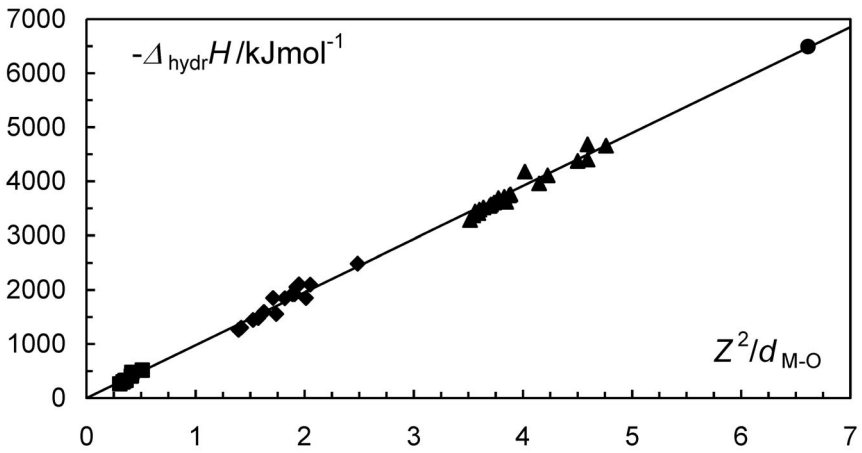

Fig. 1 Heats of hydration of some metal ions, $-\Delta_{hydr}H$, as function Z^2/d_{M-O}; squares = monovalent; diamonds = divalent; triangles = trivalent; circles = tetravalent ions. The heats of hydration are collected from refs. [1,2], and the M–O bond distances are summarized in Table 1.

As the M–O bonds are mainly of electrostatic character, the coordination number of the hydrated metal ions is expected to be determined by the ratio of the ionic radius of the metal ion and the radius of the water oxygen atom [3]; the size of the water oxygen atom at coordination to metal ions has been determined to be 1.34 Å [4]. It is therefore expected that metal ions with an ionic radius smaller than 0.55 Å (the lower-limiting radius ratio, $r_{ion}/r_{O\ in\ H_2O}$, for the octahedron is 0.414) is expected to be tetrahedral, metal ions with an ionic radius in the range 0.55–0.98 Å (the upper-limiting radius ratio of the octahedron and the lower-limiting radius ratio of eight-coordination is 0.732) are expected to be octahedral, while metal ions with an ionic radius larger than 0.98 Å are expected to be eight-coordinate or

have an even higher coordination number. The preferred coordination figures are those with high symmetry and minimized ligand–ligand repulsion. The expected coordination figure for four-coordination is therefore the tetrahedron, for six-coordination the octahedron, for eight-coordination the square antiprism and for nine-coordination the tricapped trigonal prism, Fig. 2. However, several metal ions do not display these regular structures due to specific electronic structure, strong ability to form covalent interactions, or strong tendency to hydrolysis, causing formation of cationic oxometal ions.

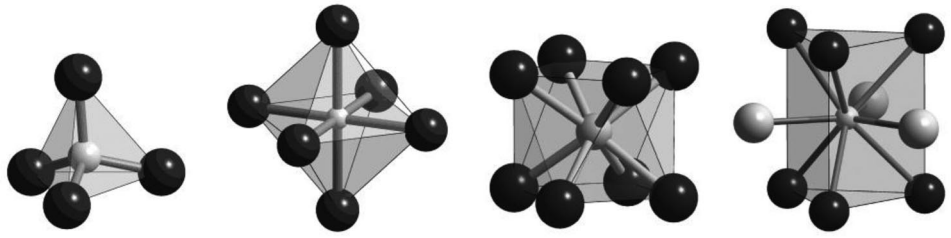

Fig. 2 Basic models for tetrahedron, octahedron, square antiprism, and tricapped trigonal prism.

SIZE OF A METAL ION

It is important to stress that a metal ion does not have a given ionic radius as it depends on the number of ligands clustered around it. Certain metal ions have a certain strongly preferred coordination number and figure due to electronic reasons, while the majority of the metal ions cluster the maximum number of ligands sterically possible around them with the ligand–ligand repulsion taken into account. This means that the coordination number will be largely determined by the ratio of the metal ion radius and the radius of the coordinating atom(s) in the ligands. The radius of the oxygen atom in coordinated water molecules, 1.34 Å [4], can be used for most monodentate oxygen donor solvents [5], except tetrahydrofuran (THF) and other ethers [6].

OVERVIEW OF THE STRUCTURE OF HYDRATED METAL IONS

The M–O bond distances used to determine the ionic radii of metal ions and anions are preferably determined in aqueous solution to avoid the influence of lattice and other packing energies. Furthermore, information of second and possible third hydration shells can only be obtained in aqueous solution. Several examples have been found where the coordination number of the first hydration sphere of a hydrate may be different in solid salts and in aqueous solution as, e.g., found for bismuth(III) [7]. For several metal ions with low charge density, crystallization takes place without the ion being hydrated, as for the alkali and silver ions [8,9]. It is therefore not possible to extrapolate the hydrate structure of several metal ions in aqueous solution from solid-state structures. The structures of most hydrated metal ions in aqueous solution have been studied by extended X-ray absorption fine structure (EXAFS), large-angle X-ray scattering (LAXS), and/or large-angle neutron scattering (LANS).

The hydrated alkali and alkaline earth metal ions display the expected coordination numbers and configurations based on their ionic radii. The coordination numbers and figures of the alkali metal ions (d^0) are still not characterized in aqueous solution in such a way that certain values can be given even though the lithium and sodium ions seem to be octahedral [10–12], the potassium [10–12], and rubidium [13] ions square antiprismatic, and the cesium ion probably 12-coordinated [10–12]. The alkaline earth metal ions (d^0) have much more well-defined hydrate structures, with beryllium(II) being tetrahedral [14,15], magnesium(II) octahedral [10,11], and calcium(II), strontium(II), and barium(II) square antiprismatic [10,11,14–16]. The trivalent group 3 metal ions (d^0) show a more scattered pattern, with the scandium(III) ion being eight-coordinate in a tricapped trigonal prismatic fashion due to partial

water deficit in two of the three capping positions as will be discussed below for the heavier lanthanoid(III) ions [17,18]. The larger yttrium(III) and lanthanum(III) ions are eight- and nine-coordinate in square antiprismatic and tricapped trigonal prismatic configuration, respectively [17,19,20]. In group 4, the hydrated titanium(III) ion (d^1) is reported to have a slightly compressed octahedral structure [21]. Titanium(IV) (d^0) is present as an oxo ion, titanyl(IV), TiO^{2+}, as it has too high charge density to resist hydrolysis in water independent of the level of acidity. The tetravalent zirconium and hafnium ions (d^0) are square antiprismatic as expected from their ionic radii, even though they are extremely prone to hydrolyze to tetrameric $[M_4(OH)_8(H_2O)_{16}]^{8+}$ ions [22]. In group 5 only, vanadium has cationic chemistry in aqueous solution. The hydrated vanadium(II) and vanadium(III) ions (d^1 and d^2, respectively) are both octahedral based on structure in the solid-state and theoretical simulations [8,9,23], but it has not yet been confirmed by experimental structural studies in aqueous solution. The vanadium(IV) or vanadyl(IV), VO^{2+}, and vanadium(V) or vanadyl(V), VO_2^+, ions are present as cationic oxo ions for the same reason as the titanyl(IV) ion. The group 6 metals chromium and molybdenum have cationic chemistry in the oxidation states +II (d^4) and +III (d^3). The chromium(II) ion has Jahn–Teller distorted octahedral configuration [24], while molybdenum(II) is present as a dimer with a quadruple bond between the molybdenum(II) ions, and each molybdenum(II) is hydrated with approximately four water molecules [25]. The hydrated chromium(III) ion has a well-established octahedral structure in aqueous solution [26], while the hydrated molybdenum(III) ion is found to be a regular octahedron in the solid state [27], while in aqueous solution strong hydrolysis is reported. The hydrated metal ions in groups 7–9, manganese(II) (d^5), iron(II) (d^6), iron(III) (d^5), ruthenium(II) (d^6), ruthenium(III) (d^5), osmium(II) (d^6), cobalt(II) (d^7), cobalt(III) (d^6), rhodium(III) (d^6), and iridium(III) (d^6) have all octahedral configuration [10,11,28–34]. In group 10, the hydrated nickel(II) ion (d^8) is octahedral [35], while the hydrated palladium(II) and platinum(II) ions (d^8), previously believed to be square planar, have been shown to have strongly tetragonally elongated octahedral configuration [36–40]. In group 11, the hydrated metal ions copper(I) (d^{10}), copper(II) (d^9), silver(I) (d^{10}), and gold(III) (d^8) ions display different configurations. The hydrated copper(I) is believed to have tetrahedral configuration, but only indirect experimental indications have been presented so far [41]. The hydrated copper(II) ion has Jahn–Teller distorted octahedral configration [42–44], and the hydrated silver(I) ion display a linearly distorted configuration [45]. The hydrated zinc(II) and cadmium(II) ions (d^{10}) have regular octahedral configuration [10,11], while mercury(II) ion (d^{10}) display a distorted octahedral configuration due to second-order Jahn–Teller effects [46]. The hydrated trivalent metal ions in group 13, aluminum(III), gallium(III), indium(III), and thallium(III) (d^{10}) ions have all regular octahedral configuration [10,11,26,47,48], while the structure of the hydrated thallium(I) ion ($d^{10}s^2$) in aqueous solution is difficult to define [49]. The structure of the hydrated thallium(I), tin(II), and lead(II) ions ($d^{10}s^2$) is strongly affected by the lone electron pair, giving complexes with low symmetry (hemi-directed) [12,49], while the hydrated bismuth(III) ion ($d^{10}s^2$) has a regular square antiprismatic configuration, showing that the lone electron pair of this triply charged ion has no stereochemical effect, giving a symmetric hydrate complex (holo-directed) [7]. The hydrated lanthanoid(III) ions all have basic tricapped trigonal prismatic structure in aqueous solution. The hydrates of the lanthanum(III) ion and the lightest lanthanoid(III) ions, Ce–Nd, all have a regular tricapped trigonal structure with the capping water molecules at ca. 0.10 Å longer bond Ln–O distance than to the water molecules forming the prism [17,50,51]. Starting from samarium(III), the three capping water molecules will not be equally strongly bound, but the basic tricapped trigonal prism is still maintained [50,51]. Starting at holmium(III), the bond strength of the two weakly bound capping water molecules has decreased to such a degree that full occupancy cannot be maintained, thus, there is a water deficit in comparison to the basic configuration [50,51]. The hydrated actinoid(III) and actinoid(IV) ions seem all to be nine-coordinate, probably tricapped trigonal prismatic configuration, in aqueous solution, even though some structures are only determined in the solid state so far [52–61]. The structures of the hydrated lanthanoid(III), actinoid(III), and actinoid(IV) ions are discussed in more detail below. The hydrated dioxouranium(VI) or

uranyl(VI) ion; UO_2^{2+} has a linear O=U=O entity with five water molecules binding to uranium in a pentagonal fashion [62].

An overview of mean bond distance, ionic radius, and configuration of the hydrated metal ions is given in Table 1, and the configuration of the most common oxidation state in aqueous solution with well-defined high symmetry is given in their respective position in the periodic table of the elements in Fig. 3.

Table 1 Overview of M–O bond distance, calculated ionic radius, the ionic radius reported by Shannon [63], and the configuration of hydrated metal ions in aqueous solution.

Aqua complex	M–O distance	M^{n+}'s ion radius/Å	Shannon	Configuration	Refs.
$Li(H_2O)_4^+$	1.95	0.61	0.59	Tetrahedron	8–11
$Li(H_2O)_6^+$	2.10	0.76	0.76	Octahedron	8–11
$Na(H_2O)_6^+$	2.43	1.09	1.02	Octahedron	8–12
$K(H_2O)_8^+$	2.84*	1.50*	1.51	Square antiprism	8–12
$Rb(H_2O)_8^+$	2.97	1.63	1.61	Square antiprism	13
$Cs(H_2O)_{12}^+$	3.25*	1.91*	1.88	12-coordination	10–12
$Cu(H_2O)_4^+$	2.14	0.80	0.60	Tetrahedron, extrapolated	41
$Ag(H_2O)_4^+$	2.32 + 2.54	0.98 + 1.2	1.00	Distorted tetrahedron	45
$Be(H_2O)_6^{2+}$	1.615	0.275	0.27	Tetrahedron	10,11
$Mg(H_2O)_6^{2+}$	2.10	0.76	0.72	Octahedron	10,11
$Ca(H_2O)_8^{2+}$	2.46	1.12	1.12	Square antiprism	15
$Sr(H_2O)_8^{2+}$	2.62	1.28	1.26	Square antiprism	16
$Ba(H_2O)_8^{2+}$	2.82	1.48	1.42	Square antiprism	16
$Eu(H_2O)_8^{2+}$	2.584	1.24	1.25		64
$V(H_2O)_6^{2+}$	2.14	0.80	0.79	Octahedron, blue	8,9*
$Cr(H_2O)_6^{2+}$	1.99 + 2.3	0.65 + 0.96	0.73 (LS)	Octahedron (JT), light blue	24
$Mn(H_2O)_6^{2+}$	2.20	0.86	0.830 (HS)	Octahedron, pale pink	10,11
$Fe(H_2O)_6^{2+}$	2.12	0.78	0.780 (HS)	Octahedron, pale green	10,11
$Co(H_2O)_6^{2+}$	2.08	0.74	0.745 (HS)	Octahedron, red	10,11
$Co(H_2O)_6^{3+}$	1.87	0.53	0.545 (LS)	Octahedron, blue	10,11*
$Ni(H_2O)_6^{2+}$	2.055	0.715	0.690	Octahedron, green	35
$Cu(H_2O)_6^{2+}$	1.96 + 2.28	0.62 + 0.94	0.73	Octahedron (JT), blue	42–44
$Zn(H_2O)_6^{2+}$	2.08	0.74	0.74	Octahedron	10,11
$Rh(H_2O)_6^{3+}$	2.04	0.70	0.665	Octahedron, pale yellow	32,33
$Pd(H_2O)_4^{2+}$	2.01+2.75	0.67	0.64	Square-planar, pale yellow	36
$Pt(H_2O)_4^{2+}$	2.01+2.75	0.65	0.60	Square-planar, pale yellow	40
$Cd(H_2O)_6^{2+}$	2.30	0.96	0.95	Octahedron	10,11
$Hg(H_2O)_6^{2+}$	2.34	1.00	1.02	Octahedron	46
$Pb(H_2O)_6^{2+}$	2.54	1.20	1.19		12

(*continues on next page*)

Table 1 (*Continued*).

Aqua complex	M–O distance	M^{n+}'s ion radius/Å	Shannon	Configuration	Refs.
$Al(H_2O)_6^{3+}$	1.89	0.55	0.535	Octahedron	10,11
$Ga(H_2O)_6^{3+}$	1.96	0.62	0.620	Octahedron	26
$In(H_2O)_6^{3+}$	2.14	0.80	0.80	Octahedron	26
$Tl(H_2O)_6^{3+}$	2.22	0.88	0.885	Octahedron	47,48
$Sc(H_2O)_{8.0}^{3+}$	2.17 + 2.33	0.83 + 0.99	0.87	Tricapped trigonal prism	17,18
$Ti(H_2O)_6^{3+}$	2.03	0.69	0.67	Octahedron, violet	65,66*
$V(H_2O)_6^{3+}$	1.994	0.654	0.640	Octahedron, blue	8,9*
$Cr(H_2O)_6^{3+}$	1.96	0.62	0.615	Octahedron, blue–green	26
$Fe(H_2O)_6^{3+}$	2.00	0.66	0.645 (HS)	Octahedron, pale violet	10,11
$Y(H_2O)_8^{3+}$	2.36	1.02	1.019	Square antiprism	9
$La(H_2O)_9^{3+}$	2.52 + 2.64	1.18 + 1.30	1.216	Tricapped trigonal prism, colorless	50,51
$Ce(H_2O)_9^{3+}$	2.54	1.20	1.196	Tricapped trigonal prism, pale red	50,51
$Pr(H_2O)_9^{3+}$	2.50	1.16	1.179	Tricapped trigonal prism, pale green	50,51
$Nd(H_2O)_9^{3+}$	2.49	1.15	1.163	Tricapped trigonal prism, pale violet–red	50,51
$Sm(H_2O)_9^{3+}$	2.46	1.12	1.132	Tricapped trigonal prism, pale yellow	50,51
$Eu(H_2O)_9^{3+}$	2.425	1.085	1.062	Tricapped trigonal prism, pale reddish	50,51
$Gd(H_2O)_9^{3+}$	2.415	1.075	1.053	Tricapped trigonal prism, colorless	50,51
$Tb(H_2O)_9^{3+}$	2.39	1.05	1.040	Tricapped trigonal prism, pale pink	50,51
$Dy(H_2O)_9^{3+}$	2.37	1.03	1.027	Tricapped trigonal prism, pale yellow	50,51
$Ho(H_2O)_{8.91}^{3+}$	2.36	1.02	1.015	Tricapped trigonal prism, pale yellow	50,51
$Er(H_2O)_{8.96}^{3+}$	2.35	1.01	1.004	Tricapped trigonal prism, pale pink–red	50,51
$Tm(H_2O)_{8.7}^{3+}$	2.33	0.99	0.994	Tricapped trigonal prism, pale green	50,51
$Yb(H_2O)_{8.5}^{3+}$	2.32	0.98	0.985	Tricapped trigonal prism, colorless	50,51
$Lu(H_2O)_{8.2}^{3+}$	2.31	0.97	0.977	Tricapped trigonal prism, colorless	50,51
$Bi(H_2O)_8^{3+}$	2.41	1.07	1.17	Square antiprism	7
$Pu(H_2O)_9^{3+}$	2.48 (+ 2.57)	1.14 (+ 1.23)		9-coordination, violet	52,53
$Am(H_2O)_9^{3+}$	2.48 (+ 2.58)	1.14 (+ 1.24)		9-coordination, pink	52,54
$Cm(H_2O)_9^{3+}$	2.45 (+ 2.55)	1.11 (+ 1.21)		9-coordination, pale green	52,54,55

(*continues on next page*)

Table 1 (*Continued*).

Aqua complex	M–O distance	M^{n+}'s ion radius/Å	Shannon	Configuration	Refs.
$Zr(H_2O)_8^{4+}$	2.19	0.85	0.83	Square antiprism	22
$Hf(H_2O)_8^{4+}$	2.16	0.82	0.83	Square antiprism	22
$Ce(H_2O)_8^{4+}$	2.41	1.07	0.97	Square antiprism, yellow	12
$Th(H_2O)_9^{4+}$	2.45	1.11	1.13	Tricapped trigonal prism	52
$U(H_2O)_9^{4+}$	2.42	1.08	1.05	9-coordination, green	56,57
$Np(H_2O)_9^{4+}$	2.40	1.06		9-coordination, yellow–green	58,59
$Pu(H_2O)_9^{4+}$	2.39	1.05		9-coordination, brown	60,61
$Hg_2(H_2O)_6^{2+}$	2.25	0.91	0.97	Tetrahedron, Hg–Hg = 2.52 Å	67
$Mo_2(H_2O)_6^{4+}$	2.25	0.78		Tetrahedron, red, Mo–Mo = 2.12 Å	25
$TiO((H_2O)_5^{2+}$	(2.20) + 2.34	0.84		Square antiprism	12
$VO(H_2O)_5^{2+}$	(1.59) + 2.03 + 2.20	0.69 + 0.86		Distorted pyramid, blue	12
$VO_2(H_2O)_4^{+}$	(1.7) + 2.00 + 2.2	0.66 + 0.86		Distorted octahedron, yellow	12
$UO_2(H_2O)_5^{2+}$	(1.70) + 2.42	1.08		Distorted pentagonal bipyramid, yellow	62

*Data based on structures in the solid state.

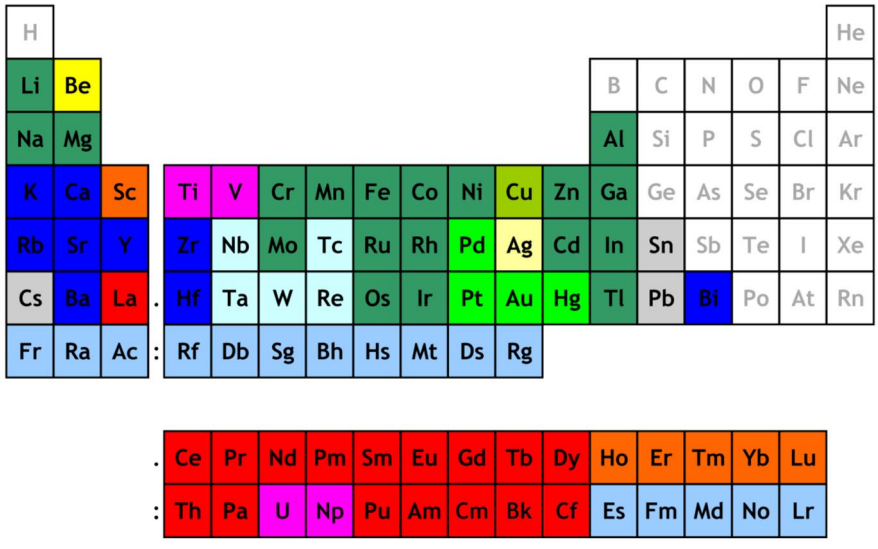

Fig. 3 Periodic table showing the basic configuration of the hydrates of the metal ions in their most common oxidation state; yellow = tetrahedron; light yellow = distorted tetrahedron; dark green = octahedron; yellowish green = Jahn–Teller distorted octahedron; bright green = PJTE distorted octahedron; blue = square antiprism; red = tricapped trigonal prism; orange = distorted tricapped trigonal prism with water deficit; magenta = oxo-metal ion; gray = other; grayish blue = metals lacking cationic chemistry in water; and light blue = configuration not established.

STRUCTURE OF METAL IONS WITH LOW SYMMETRY

Jahn–Teller distorted hydrated metal ions, chromium(II) and copper(II)

Theoretical consideration of how six ligand atoms influence the electron structure of d^4 and d^9 ions shows that certain deformations become more stable than the regular octahedral configuration [68]. For a free hexa-coordinated complex, as for the hydrated chromium(II) and copper(II) ions in aqueous solution, the Jahn–Teller theorem predicts in the O_h point group strong vibronic coupling between electronic and nuclear motion conveyed by normal vibrational modes belonging to the E_g symmetry species. The nuclear motion in the mean field of the electrons can be described by an adiabatic potential energy surface without mixing of different electronic states with three equivalent energy minima symmetrically distributed around the energy maximum at the origin corresponding to the regular octahedral configuration [68]. The minima occur for tetragonal displacements of the nuclei along the three four-fold axes of the octahedral configuration, leading to two longer axial and four shorter equatorial bond distances. Interconversion with pulsating motions of the ligand atoms takes place between the three differently oriented elongated configurations with a rate depending on the depth of the corresponding minima. There is also a weak correlation between the elongation and the strength of the vibronic coupling [68].

The structure of the hydrated copper(II) ion in aqueous solution has been debated intensively in recent years. It is, however, difficult to draw a clear conclusion as the interaction in the axial position is very weak, and the color of copper(II) complexes with Jahn–Teller distorted octahedral and tetragonally distorted square-pyramidal are pale blue, while four- and five-coordinated complexes with oxygen donor ligands are green. In the solid state, a very large majority of the reported structures display a Jahn–Teller distorted structure with mean Cu–O bond distances of 1.975 and 2.35 Å in the equatorial and axial positions, respectively [8,9]. A limited number of solid-state structures contain penta-aquacopper(II) complexes in distorted square-pyramidal configuration with the axial position at the same distance as found in the six-coordinate Jahn–Teller distorted complexes [69–74], and only one penta-aquacopper(II) complex with trigonal bipyramidal configuration [75], and one tetra-aquacopper(II) complex with square-planar configuration [76] are reported in the solid state. Pasquarello et al. proposed some years ago that the hydrated copper(II) ion is five-coordinate in aqueous solution [77], a view which has been supported by theoretical simulations and EXAFS/XANES studies [78,79]. EXAFS and LAXS studies did, however, give physically unrealistic Debye–Waller factors with on average only one water in the axial positions, supporting a Jahn–Teller distorted octahedral configuration [42]. Another EXAFS/XANES study concluded that it is not possible to distinguish between four-, five-, and six-coordinate hydrate structures of copper(II) [43], and a recent theoretical simulation showed that the energetic difference between five- and six-coordination is very small (ca. 5 kJ/mol) supporting co-existence in aqueous solution [44]. It is not possible from the present experimental or theoretical simulation data to unambiguously determine if the hydrated copper(II) ion is five- or six-coordinated or if they co-exist in aqueous solution, but five-coordination in trigonal bipyramidal fashion and four-coordination can be ruled out as copper(II) complexes in these configurations have a different color, green [8,9]. However, it is a striking fact that the number of six-coordinate copper(II) aqua complexes in the solid state is much larger than the number of five-coordinate, in spite of the much lower water activity at the formation of a solid phase than in aqueous solution.

The structure of the hydrated copper(II) ion has been reported in numerous studies in both aqueous solution [10,11,42] and the solid state [8,9,42]. The mean Cu–O bond distance to the equatorially bound water molecules is 1.975 Å, and ca. 2.35 Å to the axially bound ones. However, the crystallographic studies of the solids $[Cu(H_2O)_6]SiF_6$ and $[Cu(H_2O)_6](BrO_3)_2$ show a regular octahedral coordination of six water molecules around copper(II) [80,81]. It has been shown by a combined EXAFS and crystallographic study that the individual hydrated copper(II) complexes have the expected Jahn–Teller distortion, but due to a random distribution of the direction of axial water molecules, the overall mean symmetry becomes higher than the symmetry of the individual complexes [43]. This is

certainly also true for the structure of $[Cr(H_2O)_6]SiF_6$ [82], which is isostructural with $[Cu(H_2O)_6]SiF_6$ even though it has not been experimentally proven.

The hydrated chromium(II) ion displays as expected a significantly tetragonally elongated octahedral structure with four strongly bound water molecules in a square plane, and with two water molecules in the apical position at much longer bond distance. Only one EXAFS study has been reported on the hydrated chromium(II) ion with a Cr–O bond distance of 2.08 Å in the equatorial positions, while no water molecules in the apical positions were detected [24]. This value is in excellent agreement with the structure of the chromium(II) ion in solid $(NH_4)_2[Cr(H_2O)_6](SO_4)_2$, where the Cr–O bond distance to the water molecules in the apical position are ca. 2.34 Å [83,84].

Electronically affected metal ions, mercury(II), silver(I), palladium(II), and platinum(II)

The hydrated mercury(II) ion is six-coordinate in a somewhat distorted fashion in aqueous solution as well as in some solid salts [46,85]. Mercury(II) has also a strong tendency to form colinear complexes as, e.g., seen in the hydrate structure of $[Hg(H_2O)_2(\mu_2\text{-}CF_3SO_3)_2]_\infty$ [86], where the water molecules are strongly bound while the trifluoromethanesulfonate oxygens are weakly bound in a strongly linearly distorted octahedron. The destabilization of regular six-coordinated mercury(II) complexes, including small monodentate ligands, is often attributed to a contribution of the mercury(II) $5d_{z2}$ atomic orbital to the bonding molecular orbitals by vibronic coupling of pseudo-degenerate electronic states in a so-called pseudo Jahn–Teller effect (PJTE) [87–90]. Another explanation of the strong preference for linear two-coordination with strong covalent contribution for the heavy d^{10} ions mercury(II) and gold(I) has also been suggested. Relativistic spin-orbit coupling would split the three 6p orbitals and induce lower energy for one $6p_{1/2}$ orbital in relation to two degenerate $6p_{3/2}$ orbitals, and the increased closeness of the 6s and 6p valence states would thus promote sp hybridization [91,92]. However, while relativistic effects certainly contribute to the special properties of the heaviest atoms, this suggestion is not consistent with the similar, albeit weaker tendency to linear two-coordination of the lighter d^{10} ions silver(I) and copper(I), also with close valence shell states, while no similar tendency of linear coordination is found for cadmium(II). In the hydrated mercury(II) ion, four water molecules are slightly more strongly bound, ca. 0.05 Å shorter than the remaining two in the axial positions.

The structure of the hydrated silver(I) ion in aqueous solution has been studied by LAXS, EXAFS, and LANS. It was agreed that the hydrated silver(I) ion binds four water molecules in tetrahedral configuration in aqueous solution [10,11]. However, there was a general trend in the reported mean Ag–O bond distances in the hydrated silver(I) ion depending on the method used. LAXS and LANS on one hand give a mean Ag–O bond distance of 2.38–2.45 Å [10,11,93–95] while EXAFS on the other gives mean Ag–O bond distances of 2.31–2.36 Å [96–98]. The LAXS and EXAFS techniques are complementary, and the same result should be obtained if the model applied is the correct one [16]. In a recent study, new LAXS and EXAFS data were collected and by applying the regular tetrahedral model of the hydrated silver(I) ion the previously reported results were reproduced [45]. A molecular dynamics simulation based on ab initio quantum mechanical forces with molecular dynamics proposes that the silver(I) ion has an irregular-shaped first hydration shell with a mean coordination number of about 5.5 in aqueous solution (0.1096 mol dm^{-3}) [99], but with Ag–O bond distances much longer than the experimentally obtained ones [100]. By applying a non-regular model for the hydrated silver(I) ion with two water molecules bound at short distance, 2.32 Å and 2–4 water molecules at much longer distance, ca. 2.5 Å, very good fits were obtained for both LAXS and EXAFS data [45]. This shows that the hydrated silver(I) ion has an even stronger PTJE than mercury(II), probably due to the lower charge.

The structure of the hydrated palladium(II) and platinum(II) ions in aqueous solution were for a long time believed to be square-planar, even though reaction mechanisms have required five- or six-coordinated transition states to explain the observed kinetics [101]. Recent EXAFS and simulation studies have shown the presence of two very weakly bound water molecules in the axial positions [36–40]. The

Pd/Pt-water interactions in the axial positions are very weak, being ca. 0.7 Å longer than the equatorially bound water molecules [36,40].

Metal Ions with lone electron pair, thallium(I), tin(II), and lead(II) and bismuth(III)

The thallium(I), tin(II), lead(II), and bismuth(III) ions have all $d^{10}s^2$ electron configuration, where the lone s^2 electron pair may affect the stereochemistry of the complexes. The configuration of the complexes of these ions depends on the character of the lone s electron pair. According to the valence bond theory, this inert pair can either occupy a hybrid orbital formed by mixing the s and p orbitals on the metal ion (stereochemically active character) or be an s^2 pair (inactive character). A hybrid orbital with a lone s electron pair is considered as an additional ligand in the coordination sphere. However, in the heart of molecular orbital theory, it is regarded that the classical concept of s and p orbital hybridization on the metal ion is not correct and the stereochemical activity of the s^2 electron pair is the result of the anti-bonding metal ion–donor atom interactions [101]. This inert electron pair is characteristic for the p-block elements. The role of the lone electron pair on the metal ions has been considered and analyzed in several studies [103,104]. Two general structural types of configuration of the metal ions is observed, hemi-directed, with a gap for the lone electron pair, and holo-directed, without a gap, as presented by Shimoni-Livny et al. [104].

The hydrated thallium(I) ion has clear signs of a stereoactive s^2 lone electron pair, with two different Tl–O bond distances, 2.7 and 3.2 Å. However, it has not been possible to determine neither the number of distances nor the configuration of the hydrated thallium(I) ion in aqueous solution [49]. There are no crystal structures containing hydrated thallium(I) ions reported [8,9].

The stereochemical effects in the hydrated tin(II) and lead(II) ions complexes are clearly seen in a number of complexes, with the lone electron pair occupying nearly half of the sphere of the ion [8,9]. The hydrated tin(II) ion is hemi-directed with the water molecule *trans* to the lone pair more strongly coordinated than the four water molecules in the equatorial plane, 2.20 and 2.34 Å, respectively [12], in aqueous solution. The solid monoaqua(bis(μ_2-trifluoromethanesulfonato)lead(II), is holo-directed, Fig. 4, while solid lead(II) perchlorate sesquihydrate is clearly hemi-directed [12]. When lead(II) binds six oxygen ligands in a holo-directed configuration, the mean Pb–O bond distance is significantly shorter than in six-coordinated hemi-directed complexes (which become at least seven-coordinated when the space of the lone pair is included); the mean Pb–O bond distances are 2.48 and 2.55 Å, respectively [8,9]. The mean Pb–O bond distance in the hydrated lead(II) ion in aqueous solution is 2.54 Å, and without any observable inner-core multiple scattering in the EXAFS data, strongly indicating a hemi-directed six-coordinate complex [12].

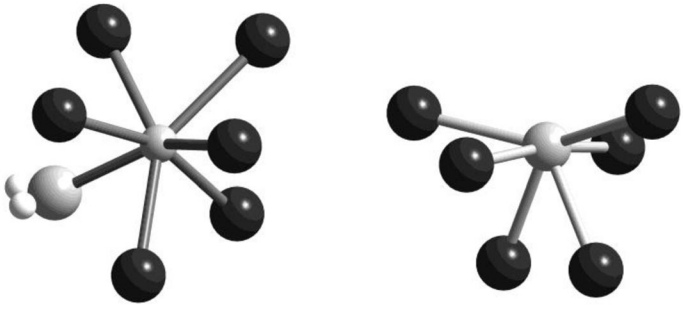

Fig. 4 Structure of $[Pb(H_2O)(CF_3SO_3)_2]$ in solid-state, holo-directed, and the hydrated lead(II) ion in aqueous solution, hemi-directed.

The bismuth(III) ion has also $d^{10}s^2$ electron configuration, but here the stereochemical effects are suppressed probably due to the high charge density yielding no gap for the lone electron pair (holo-directed) [8,9]. The hydrated bismuth(III) ion is eight-coordinate in distorted square antiprismatic fashion in aqueous solution, while in the solid trifluoromethanesulfonate salt it has tricapped trigonal prismatic configuration.

Hydrated lanthanoid(III) and scandium(III) ions

The hydrated lanthanoid(III) and scandium(III) ions all have a basic tricapped trigonal configuration in aqueous solution. The hydrates of the lanthanum(III) ion and the lightest lanthanoid(III) ions, Ce–Nd, all have a regular tricapped trigonal structure in both aqueous solution and the solid state [50,51], with the capping water molecules at ca. 0.10 Å longer bond Ln–O distance than to the water molecules forming the prism. The ionic radius of the lanthanoid(III) ions decreases with increasing atomic number due to the lanthanoid contraction. This will, in principle, not affect the structure of the prism, which also decreases in size when the ionic radius of the metal ion decreases, but the more weakly bound capping positions are strongly affected. Starting from samarium(III), the three capping water molecules will not be equally strongly bound. Instead, one of the capping water molecules will be more strongly bound (at shorter bond distance) than the remaining two (Fig. 5). This effect is small for samarium(III), but increases step by step with increasing atomic number in the lanthanoid series. Starting at holmium(III), the bond strength of the two weakly bound capping water molecules has decreased to such a degree that full occupancy cannot be maintained, thus, there is a water deficit in comparison to the basic configuration (Fig. 5). The water deficit and the difference between the strongly bound capping water molecule and the more weakly bound ones increases from holmium(III) to lutetium(III). The hydrated lutetium(III) ion has on average 2.2 water molecules in the capping positions with one strongly bound one at 2.39 Å, and on average 1.2 water molecules in the two remaining capping positions at ca. 2.55 Å. The even smaller scandium(III) ion binds eight water molecules in both aqueous solution and solid state

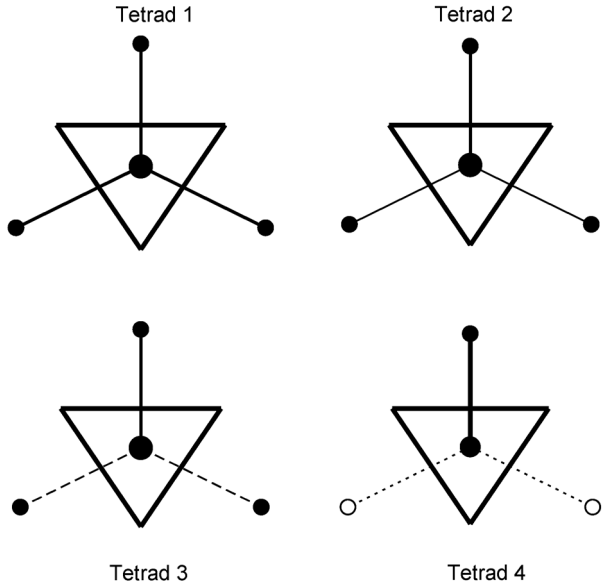

Fig. 5 Schematic illustration of the bond strength of the capping water molecules of the hydrated lanthanoid(III) ions in aqueous solution in the four tetrads. The line thickness represents the bond strength, and an open circle a less than fully occupied site; tetrad 1 = La-Nd, tetrad 2 = Pm-Gd, tetrad 3 = Tb-Ho, and tetrad 4 = Er-Lu.

in the same way as described for the hydrated lutetium(III) ion (Fig. 6), but with on average only one water molecule in the two weakly binding capping positions [50]. The reason why the heavier lanthanoid(III) ions and scandium(III) ion can maintain the tricapped trigonal configuration in spite of the water deficit and that the metal ions are obviously too small for that configuration is most probably the extensive hydrogen bonding supporting this configuration in aqueous solution and the solid state.

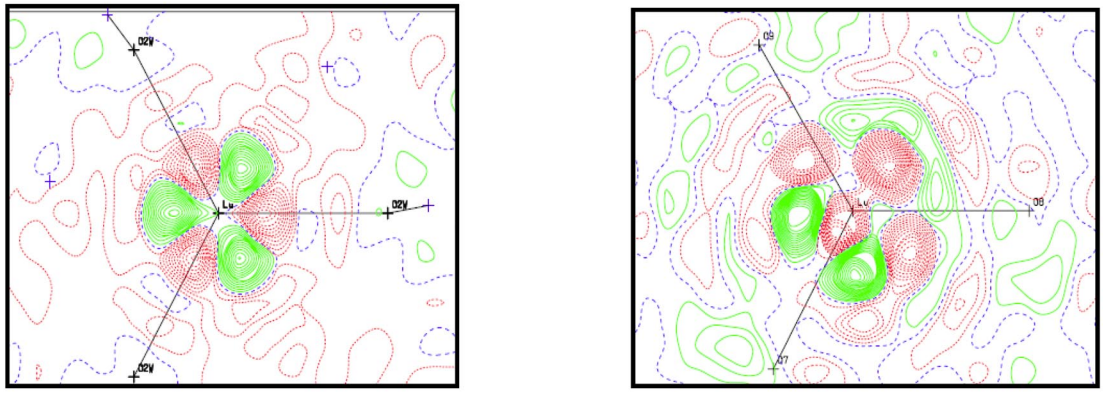

Fig. 6 Electron density map of $[Lu(H_2O)_{8.2}](CF_3SO_3)_3$ at room temperature (left) and 100 K (right). At room temperature, the strongly bound capping water molecule is randomly oriented giving a three-hold symmetry around lutetium. On the other hand, at 100 K the position of the strongly bound capping water molecule, O7, is well defined and Lu moves to a position between O7 and O8 when position O9 is empty or between O7 and O9 when O8 is empty (green denotes higher electron density and red lower electron density than accounted for by the structural model, see ref. [28] for further details).

Hydrated actinoid(III) and actinoid(IV) ions

The structures of the hydrated actinoid(III) and actinoid(IV) ions have been studied in aqueous solution by means of EXAFS, which means that only bond distances can be determined accurately. Furthermore, a number of hydrate structures have been reported in the solid state. In order to determine as accurately as possible the coordination number in the hydrates in aqueous solution, the structures of complexes of monodentate oxygen donor ligands determined crystallographically were summarized. This summary showed that the bond distance for every coordination number is quite narrow and hardly overlaps between each other. The mean An–O bond distances as a function of coordination number for actinoid(IV) ions are given in Fig. 7 [52].

Of the trivalent actinoid ions, plutonium(III), americium(III), and curium(III) have been studied in aqueous solution [52]. The mean An–O bond distances reported, 2.48, 2.48, and 2.45 Å, is very close to the An–O bond distance to the capping water molecules in $[An(H_2O)_9](CF_3SO_3)_3$ [53–55], while capping water molecules (ca. 2.57 Å in the solids) were not observed in aqueous solution [52,54].

The structure of the hydrated thorium(IV) ion has been shown to be nine-coordinate, most probably in tricapped trigonal prismatic fashion, in aqueous solution, with a mean Th–O bond distance of 2.45 Å [56]. The U–O bond distance in the hydrated uranium(IV) ion has been determined to be 2.42 Å in two separate studies, strongly indicating a nine-coordination, see Fig. 7 [56,57], probably in tricapped trigonal prismatic configuration. EXAFS studies of hydrated neptunium(IV) and plutonium(IV) ions in acidic aqueous solution report An–O bond distances of 2.40 and 2.39 Å, respectively [58–61], showing that also these ions seem to be nine-coordinate in aqueous solution, Fig. 7.

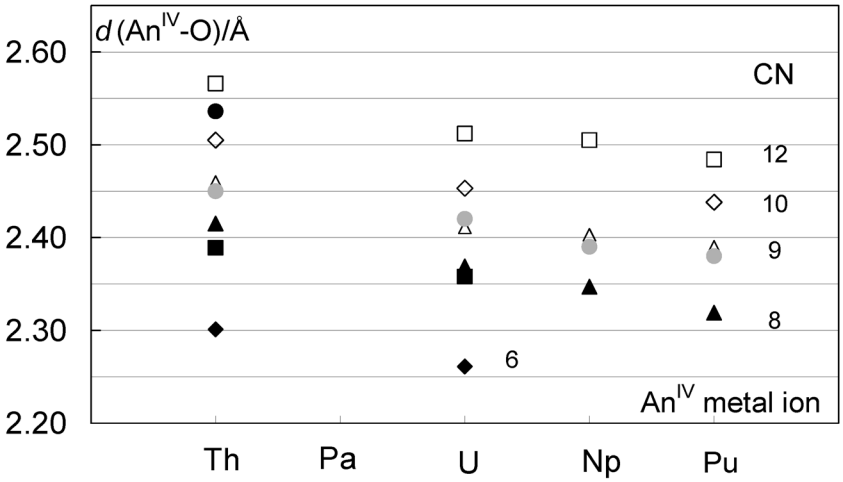

Fig. 7 The actinoid(IV)-oxygen bond distances and coordination numbers of the actinoid(IV) structures with monodentate ligands reported in ref. [56]. The gray circles mark the An–O bond distances reported in aqueous solution, showing that the studied hydrated actinoid(IV) ions are all nine-coordinated, most probably in tricapped trigonal prismatic fashion, in aqueous solution.

Oxo-metal ions, TiO^{2+}, VO^{2+}, VO_2^+, UO_2^{2+}

Small highly charged metal ions such as titanium(IV), vanadium(IV), vanadium(V), and uranium(VI) have very high charge density, and it is not possible to avoid hydrolysis reactions in aqueous solution. As a result, the stable form of these ions is oxometal ions in aqueous solution where the charge density is highly reduced. The structures of the hydrated oxometal ions are very much affected by the strongly bound oxo group(s). The structures of hydrated titanyl(IV) and vanadyl(IV) ions have the same principle structure with a basic octahedral configuration with the water molecule *trans* to oxo group very weakly bound, and with the four equatorial water molecules in a plane somewhat below metal ion, Fig. 8. The hydrated vanadium(V) ion has a basic octahedral configuration and an unusual configuration with two oxo groups bound in *cis*-configuration. The water molecules *trans* to the oxo groups are weakly bound, while the remaining two water molecules, *cis* to the oxo groups, have intermediate V–O bond distances, Fig. 9. The hydrated uranyl(VI) ion binds two oxo groups in *trans* configuration, and perpendicular to the O=U=O entity five water molecules are bound to uranium [62].

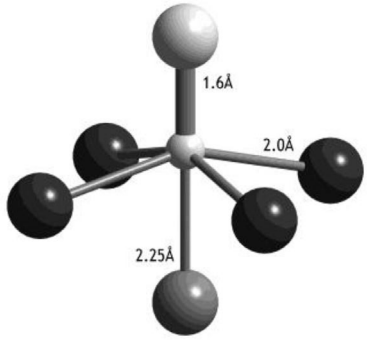

Fig. 8 Structure of $VO(H_2O)_5^{2+}$ in aqueous solution, ref. [12].

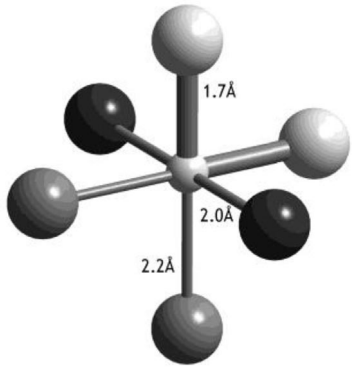

Fig. 9 Structure of $VO_2(H_2O)_4^+$ in aqueous solution, ref. [12].

IONIC RADII OF HYDRATED METAL IONS

The configurations and M–O bond distances in most metal ions in aqueous solution are well established as summarized in Table 1. Using this information, the ionic radii of these metal ions in the configuration they have in aqueous solution can be derived from the M–O bond distance and the size of the oxygen atom in coordinated water molecules, 1.34 Å [4]. The classic ionic radii of metal ions reported by Shannon, and Shannon and Prewitt [63], are in most cases in excellent agreement with the ionic radii derived from M–O bond distances and the size of the oxygen in coordinated water molecules, Table 1. However, in some cases they do not, mainly due to the fact that Shannon used oxide and fluoride structures where accurate data were lacking for some metal ions for the coordination number/configuration observed in the hydrated metal ions in aqueous solution [5]. The ionic radii given in Table 1 are probably the most accurate ones available as lattice effects are affecting the values proposed by Shannon.

ACKNOWLEDGMENTS

The financial support for this project from the Swedish Research Council is gratefully acknowledged. Dr. Daniel Lundberg is acknowledged for constructing the figures.

REFERENCES

1. D. R. Rosseinsky. *Chem. Rev.* **65**, 467 (1965).
2. C. G. Phillips, R. J. P. Williams. *Inorganic Chemistry*, Vol. 1, p. 161, Clarendon Press, New York (1965).
3. R. G. Pearson. *J. Am. Chem. Soc.* **85**, 3533 (1963).
4. J. K. Beattie, S. P. Best, B. W. Skelton, A. H. White. *J. Chem. Soc., Dalton Trans.* 2105 (1981).
5. D. Lundberg, I. Persson, L. Eriksson, P. D'Angelo, S. De Panfilis. *Inorg. Chem.* **49**, 4420 (2010).
6. R. Ireland, P. Wipf, J. Armstrong. *J. Org. Chem.* **56**, 650 (1991).
7. J. Näslund, I. Persson, M. Sandström. *Inorg. Chem.* **39**, 4012 (2000).
8. *Inorganic Crystal Structure Database* 1.4.6, Release 2009-1, FIZ Karlsruhe (2009).
9. (a) F. H. Allen. *Acta Crystallogr., Sect. B* **58**, 380 (2002); (b) *Cambridge Structure Database*, Release 2008.
10. H. Ohtaki, T. Radnai. *Chem. Rev.* **93**, 1157 (1993) and refs. therein.
11. G. Johansson. *Adv. Inorg. Chem.* **39**, 159 (1992) and refs. therein.
12. I. Persson. Unpublished data.
13. P. D'Angelo, I. Persson. *Inorg. Chem.* **43**, 3543 (2004).

14. T. Yamaguchi, H. Ohtaki, E. Spohr, G. Palinkas, K. Heinzinger, M. Probst. *Z. Naturforsch., A* **41**, 1175 (1986).
15. F. Jalilehvand, D. Spångberg, P. Lindqvist-Reis, K. Hermansson, I. Persson, M. Sandström. *J. Am. Chem. Soc.* **123**, 431 (2001).
16. I. Persson, M. Sandström, H. Yokoyama, M. Chaudhry. *Z. Naturforsch., A* **50**, 21 (1995).
17. A. Abbasi, P. Lindqvist-Reis, L. Eriksson, D. Sandström, S. Lidin, I. Persson, M. Sandström. *Chem.—Eur. J.* **11**, 4065 (2005).
18. P. Lindqvist-Reis, I. Persson, M. Sandström. *Dalton Trans.* 3868 (2006).
19. P. Lindqvist-Reis, K. Lamble, S. Pattanaik, M. Sandström, I. Persson. *J. Phys. Chem. B* **104**, 402 (2000).
20. J. Näslund, P. Lindqvist-Reis, S. Pattanaik, M. Sandström, I. Persson. *Inorg. Chem.* **39**, 4006 (2000).
21. H. Tachikawa, T. Ichikawa, H. Yoshida. *J. Am. Chem. Soc.* **112**, 977 (1990).
22. C. Hagfeldt, V. Kessler, I. Persson. *Dalton Trans.* 2142 (2004).
23. H. Loeffler, J. Iglesias Yagüe, B. M. Rode. *Chem. Phys. Lett.* **363**, 367 (2002).
24. T. Miyanaga, I. Watanabe, S. Ikeda. *Chem. Lett*. 1073 (1988).
25. S. P. Cramer, P. K. Eidem, M. T. Pafett, J. R. Winkler, Z. Dori, H. B. Gray. *J. Am. Chem. Soc.* **105**, 799 (1983).
26. P. Lindqvist-Reis, S. Diaz-Moreno, A. Munoz-Páez, S. Pattanaik, I. Persson, M. Sandström. *Inorg. Chem.* **37**, 6675 (1998), and refs. therein.
27. M. Brorson, M. Gajhede. *Inorg. Chem.* **26**, 2109 (1987).
28. D. Lundberg, A.-S. Ullström, P. D'Angelo, I. Persson. *Inorg. Chim. Acta* **360**, 1809 (2007).
29. M. Taimisto, R. Oilunkaniemi, R. S. Laitinen, M. Ahlgren. *Z. Naturforsch., B* **58**, 959 (2003).
30. S. P. Best, J. Bruce Forsyth. *J. Chem. Soc., Dalton Trans.* 3507 (1990).
31. P. Bernhard, H.-B. Bürgi, J. Hauser, H. Lehmann, A. Ludi. *Inorg. Chem.* **21**, 3936 (1982).
32. R. Caminiti, D. Atzei, P. Cucca, A. Anedda, G. Bongiovanni. *J. Phys. Chem.* **90**, 238 (1986).
33. M. C. Read, M. Sandström. *Acta Chem. Scand.* **46**, 1177 (1992).
34. R. S. Armstrong, J. K. Beattie, S. P. Best, B. W. Skelton, A. H. White. *J. Chem. Soc., Dalton Trans.* 1973 (1983).
35. O. Kristiansson, I. Persson, D. Bobicz, D. Xu. *Inorg. Chim Acta* **344**, 15 (2003).
36. T. S. Hofer, B. R. Randolf, A. Ali Shah, B. M. Rode, I. Persson. *Chem. Phys. Lett.* **445**, 193 (2007).
37. E. C. Beret, R. R. Pappalardo, N. L. Doltsinis, D. Marx, E. S. Marcos. *ChemPhysChem* **9**, 237 (2008).
38. J. Purans, B. Fourest, C. Cannes, V. Sladkov, F. David, L. Venault, M. Lecomte. *J. Chem. Phys. B* **109**, 11074 (2005).
39. F. Jalilehvand, L. J. Laffin. *Inorg. Chem.* **47**, 3248 (2008).
40. T. S. Hofer, B. R. Randolf, B. M. Rode, I. Persson. *Dalton Trans.* 1512 (2009).
41. I. Persson, J. E. Penner-Hahn, K. O. Hodgson. *Inorg. Chem.* **32**, 2497 (1993).
42. I. Persson, P. Persson, M. Sandström, A.-S. Ullström. *J. Chem. Soc., Dalton Trans.* 1256 (2002) and refs. therein.
43. J. Chaboy, A. Munoz-Paez, P. J. Merkling, E. S. Marcos. *J. Chem. Phys.* **124**, 064509 (2006).
44. V. S. Bryantsev, M. S. Diallo, A. C. T. van Duin, W. A. Goddard III. *J. Phys. Chem. A* **112**, 9104 (2008).
45. I. Persson, K. B. Nilsson. *Inorg. Chem.* **45**, 7428 (2006).
46. I. Persson, L. Eriksson, P. Lindqvist-Reis, P. Persson, M. Sandström. *Chem.—Eur. J.* **14**, 6687 (2008).
47. J. Glaser, G. Johansson. *Acta Chem. Scand., Ser. A* **36a**, 125 (1982).
48. J. Blixt, J. Glaser, J. Mink, I. Persson, P. Persson, M. Sandström. *J. Am. Chem. Soc.* **117**, 5089 (1995).

49. I. Persson, F. Jalilehvand, M. Sandström. *Inorg. Chem.* **41**, 192 (2002).
50. I. Persson, P. D'Angelo, S. De Panfilis, M. Sandström, L. Eriksson. *Chem.—Eur. J.* **14**, 3056 (2008) and refs. therein
51. P. D'Angelo, A. Zitalo, V. Migliorati, G. Mancini, I. Persson, G. Chillemi. *Chem.—Eur. J.* **16** 682 (2010).
52. P. G. Allen, J. J. Bucher, D. K. Shuh, N. M. Edelstein, I. Craig. *Inorg. Chem.* **39**, 595 (2000).
53. J. H. Matonic, B. L. Scott, M. P. Neu. *Inorg. Chem.* **40**, 2638 (2001).
54. P. Lindqvist-Reis, C. Apostolidis, J. Rebizant, A. Morgenstern, R. Klenze, O. Walter, T. Fanghaenel, R. G. Haire. *Angew. Chem., Int. Ed.* **46**, 919 (2007).
55. S. Skanthakumar, M. R. Antonio, R. E. Wilson, L. Soderholm. *Inorg. Chem.* **46**, 3485 (2007).
56. N. Torapava, I. Persson, L. Eriksson, D. Lundberg. *Inorg. Chem.* **48**, 11712 (2009).
57. H. Moll, M. A. Denecke, F. Jalilehvand, M. Sandström, I. Grenthe. *Inorg. Chem.* **38**, 1795 (1999).
58. A. Ikeda-Ohno, C. Hennig, A. Rossberg, H. Fune, A. C. Scheinost, G. Bernhard, T. Yaita. *Inorg. Chem*. **47**, 8294 (2008).
59. P. G. Allen, J. J. Bucher, D. K. Shuh, N. M. Edelstein, T. Reich. *Inorg. Chem*. **36**, 4676 (1997).
60. S. D. Conradson, K. D. Abney, B. D. Begg, E. D. Brady, D. L. Clark, C. den Auwer, M. Ding, P. K. Dorhout, F. J. Espinosa-Faller, P. L. Gordon, R. G. Haire, N. J. Hess, R. F. Hess, D. W. Keogh, G. H. Lander, A. J. Lupinetti, L. A. Morales, M. P. Neu, P. D. Palmer, P. Paviet-Hartmann, S. D. Reilly, W. H. Runde, C. D. Tait, D. K. Veirs, F. Wastin. *Inorg. Chem.* **43**, 116 (2004).
61. S. D. Conradson, D. L. Clark, M. P. Neu, W. H. Runde, C. D. Tait. *Los Alamos Sci.* **26**, 418 (2000).
62. M. Åberg, D. Ferri, J. Glaser, I. Grenthe. *Inorg. Chem.* **22**, 3986 (1983).
63. (a) R. D. Shannon. *Acta Crystallogr., Sect. A* **32**, 751 (1976); (b) R. D. Shannon, C. T. Prewitt. *Acta Crystallogr., Sect. B* **25**, 925 (1969).
64. G. Moreau, L. Helm, J. Purans, A. E. Merbach. *J. Phys. Chem. A* **106**, 3034 (2002).
65. J. Sygusch. *Acta Crystallogr., Sect. B* **30**, 662 (1974).
66. M. A. S. Aquino, W. Clegg, Q.-T. Liu, A. G. Sykes. *Acta Crystallogr., Sect. C* **51**, 560 (1995).
67. J. Rosdahl, I. Persson, L. Kloo, K. Ståhl. *Inorg. Chim. Acta* **357**, 2624 (2004).
68. I. B. Bersuker. *Electronic Structure and Properties of Transition Metal Compounds*, Chaps. 7.3 and 9.4, Wiley-Interscience, New York (1996).
69. F. Bramsen, A. D. Bond, C. J. McKenzie. *Acta Crystallogr., Sect. E* **59**, i105 (2003).
70. R. Song, K. M. Kim, Y. S. Sohn. *Inorg. Chim. Acta* **304**, 156 (2000).
71. T. C. W. Mak, C. H. L. Kennard, G. Smith, E. J. O'Reilly, D. S. Sagatys, J. C. Fulwood. *Polyhedron* **6**, 855 (1987).
72. C. Yue, Z. Lin, L. Chen, F. Jiang, M. Hong. *J. Mol. Struct.* **779**, 16 (2005).
73. Y. Kajikawa, N. Azuma, K. Tajima. *Inorg. Chim. Acta* **288**, 90 (1999).
74. O. Guillou, P. Bergerat, O. Kahn, E. Bakalbassis, K. Boubekeur, P. Batail, M. Guillot. *Inorg. Chem.* **31**, 110 (1992).
75. V. Shivaiah, S. K. Das. *Angew. Chem., Int. Ed.* **45**, 245 (2006).
76. T. C. W. Mak, C. H. L. Kennard, G. Smith, E. J. O'Reilly, D. S. Sagatys, J. C. Fulwood. *Polyhedron* **6**, 855 (1987).
77. A. Pasquarello, I. Petri, P. S. Salmon, O. Parisel, R. Car, E. Toth, D. H. Powell, H. F. Fischer, L. Helm, A. E. Merbach. *Science* **291**, 856 (2001).
78. M. Benfatto, P. D'Angelo, S. D. Longa, N. V. Pavel. *Phys. Rev. B* **65**, 174205 (2002).
79. P. Frank, M. Benfatto, R. K. Szilagyi, P. D'Angelo, S. D. Longa, K. O. Hodgson. *Inorg. Chem.* **44**, 1922 (2005).
80. S. Ray, A. Zalkin, D. H. Templeton. *Acta Crystallogr., Sect. B* **29**, 2748 (1973).
81. A. C. Blackburn, J. C. Gallucci, R. E. Gerkin. *Acta Crystallogr., Sect. C* **47**, 2019 (1991).
82. F. A. Cotton, L. R. Falvello, C. A. Murillo, J. F. Quesada. *J. Solid State Chem.* **96**, 192 (1992).

83. M. A. Araya, F. A. Cotton, L. M. Daniels, L. R. Favello, C. A. Murillo. *Inorg. Chem.* **32**, 4853 (1993).
84. B. N. Figgis, E. S. Kucharski, P. A. Reynolds. *Acta Crystallogr., Sect. B* **46**, 577 (1990).
85. G. Johansson, M. Sandström. *Acta Chem. Scand., Ser. A* **32a**, 109 (1978).
86. A. Molla-Abbassi, L. Eriksson, P. Lindqvist-Reis, J. Mink, I. Persson, M. Sandström, M. Skripkin, A.-S. Ullström. *J. Chem. Soc., Dalton Trans.* 4357 (2002).
87. L. E. Orgel. *J. Chem. Soc.* 4186 (1958).
88. R. S. Nyholm. *J. Chem. Soc., Proc.* 273 (1961).
89. I. B. Bersuker. *The Jahn–Teller Effect and Vibronic Interactions in Modern Chemistry*, Chaps. 1–5, Plenum, New York (1984).
90. I. B. Bersuker, V. Z. Polinger. *Vibronic Interactions in Molecules and Crystals*, Chaps. 3 and 4, Springer-Verlag, Berlin (1989).
91. D. Strömberg, M. Sandström, U. Wahlgren. *Chem. Phys. Lett.* **172**, 49 (1990).
92. G. Meyer, P. Nockemann. *Z. Anorg. Allg. Chem*. **629**, 1447 (2003).
93. T. Yamaguchi, G. Johansson, B. Holmberg, M. Maeda, H. Ohtaki. *Acta Chem. Scand., Ser. A* **38a**, 437 (1984).
94. M. Maeda, Y. Maegawa, T. Yamaguchi, H. Wakita. *Bull. Chem. Soc. Jpn.* **52**, 2545 (1979).
95. M. Sandström, G. W. Neilson, G. Johansson, T. Yamaguchi. *J. Phys. C, Solid State Phys.* **18**, L1115 (1985).
96. T. Yamaguchi, O. Lindqvist, J. B. Boyce, T. Claesson. *Acta Chem. Scand.*, *Ser. A* **38a**, 423 (1984).
97. T. M. Seward, C. M. B. Henderson, J. M. Charnock, B. R. Dobson. *Geochim. Cosmochim. Acta* **60**, 2273 (1996).
98. S. Moreno-Diaz. Doctoral thesis, University of Seville, Seville (1998).
99. V. Dubois, P. Archirel, A. Boutin. *J. Phys. Chem. B* **105**, 9363 (2001).
100. R. Armunanto, C. F. Schwenk, B. M. Rode. *J. Phys. Chem. A* **107**, 3132 (2003).
101. Ö. Gröning, T. Drakenberg, L. I. Elding. *Inorg. Chem.* **21**, 1820 (1982).
102. A.-V. Mudring, F. Rieger. *Inorg. Chem.* **44**, 6240 (2005) and refs. therein.
103. L. Shimoni-Livny, J. P. Glusker, C. W. Bock. *Inorg. Chem.* **37**, 1853 (1998) and refs. therein.
104. D. L. Reger, T. D. Wright, C. A. Little, J. J. S. Lamba, M. D. Smith. *Inorg. Chem.* **40**, 3810 (2001).

